ELSEVIER

Journal of Biomechanics 41 (2008) 1289–1294

JOURNAL OF BIOMECHANICS

www.elsevier.com/locate/jbiomech
www.JBiomech.com

Durotaxis as an elastic stability phenomenon

Konstantinos A. Lazopoulos[a], Dimitrije Stamenović[b,*]

[a]*Mechanics Laboratory, Faculty of Applied Sciences, National Technical University of Athens, Athens, Greece*
[b]*Department of Biomedical Engineering, Boston University, 44 Cummington Street, Boston, MA 02215, USA*

Accepted 15 January 2008

Abstract

It is well documented that directed motion of cells is influenced by substrate stiffness. When cells are cultured on a substrate of graded stiffness, they tend to move from softer to stiffer regions—a process known as durotaxis. In this study, we propose a mathematical model of durotaxis described as an elastic stability phenomenon. We model the cytoskeleton (CSK) as a planar system of prestressed elastic line elements representing actin stress fibers (SFs), which are anchored via focal adhesions (FAs) at their end points to an elastic substrate of variable stiffness. The prestress in the SFs exerts a pulling force on FAs reducing thereby their chemical potential. Using Maxwell's global stability criterion, we obtain that the model stability increases as it is moved from a softer towards a stiffer region of the substrate. Numerical simulations reveal that elastic stability of SFs has a predominantly stabilizing effect, greater than the stabilizing effect of decreasing chemical potential of FAs. This is a novel finding which indicates that elasticity of the CSK plays an important role in cell migration and mechanosensing in general.

Keywords: Cell migration; Durotaxis; Cytoskeleton; Actin stress fibers; Focal adhesions; Stability; Potential; Mathematical modeling

1. Introduction

Cell migration is essential for many physiological processes including morphogenesis, wound healing and tumor metastases (cf. Ridley et al., 2003). To accomplish certain physiological tasks, cell motion must occur in a defined direction. Directional movements of cells are guided by various environmental stimuli, including substrate chemicals, light, gravity and electrostatic potential. Recent studies have revealed that cell movements are also guided by substrate rigidity—a process known as durotaxis (Lo et al., 2000; Wong et al., 2003).

It is widely accepted that cell migration relies upon forces generated within the actin cytoskeleton (CSK) and applied to the extracellular matrix via focal adhesions (FAs) (cf. Mitchison and Cramer, 1996; Pelham and Wang, 1997; Sheetz et al., 1998; Li et al., 2005). Sheetz et al. (1998) hypothesized that cell migration relies on the stabilization of FA-CSK contacts and the generation of force on those contacts to overcome the resistance to migration. They argued that the strength of FA contacts depends on the substrate rigidity and therefore, cells could use it to direct their migration. Lo et al. (2000) provided experimental evidence for the substrate rigidity-dependent cell migration, a process they referred to as durotaxis. These authors explained their findings as follows: cells send local protrusions, mainly composed of actin, to probe substrate stiffness using their contractile apparatus. Those protrusions that land on stiff substrate regions receive strong feedback and remain stable and anchored to the substrate. Those that land on soft substrate regions receive weak feedback, have mobile anchorages and become unstable. This creates a bias that guides cell movement from softer towards stiffer substrate regions.

Cells' responses to active mechanosensing of their microenvironment have been studied as elastic stability phenomena (cf. Wang, 2000; Bischofs and Schwarz, 2003; Lazopoulos and Stamenović, 2006). Bischofs and Schwarz (2003) showed that these responses could be explained from one unifying principle, namely that cells that adhere to stiffer substrates invest a smaller mechanical work by

*Corresponding author. Tel.: +1 617 353 5902; fax: +1 617 353 6766.
E-mail address: dimitrij@bu.edu (D. Stamenović).

0021-9290/$ - see front matter © 2008 Elsevier Ltd. All rights reserved.
doi:10.1016/j.jbiomech.2008.01.008

their contractile apparatus to build up a certain force than cells that adhere to softer substrates. Using a similar idea, we develop in this study a mathematical model that describes durotaxis as an elastic stability phenomenon. Since the interplay between contractile actin and FAs is essential for cell migration, we focus on the stability of a system comprised of actin stress fibers (SFs) anchored via FAs to an elastic substrate of variable stiffness. We find that the model becomes more stable when it is moved from softer towards stiffer substrate regions and less stable when it is moved from stiffer to softer substrate regions. This may explain the observation that cells always migrate in the direction of increasing substrate stiffness and never in the opposite direction (Lo et al., 2000; Wong et al., 2003).

2. Model

We model the CSK as a planar system of actin SFs, anchored at their endpoints to an elastic substrate via FAs. We assume that SFs carry initial tension that is transmitted to the substrate via FAs and balanced by substrate traction forces, as observed in living cells (Wang et al., 2001). We further assume that dimensions and elastic properties of all SFs are uniform, that dimensions and the chemical potential of all FAs are uniform, that different SFs do not share common FAs and that tension in all SFs is always the same. Taken together, these assumptions imply that properties of the network are completely determined by the properties of a single SF and the adjacent FAs. We want to show that when the model is moved from a softer towards a stiffer substrate region, it gains stability and when it is moved from the stiffer to the softer substrate region, it loses stability.

2.1. Actin stress fibers

Actin SFs are envisioned as elastic line elements which carry initial tensile stress (prestress) and prestrain. In living cells, this tension is primarily due to the action of contractile motors (Deguchi et al., 2006). In our model, tension in the SFs is generated by their passive elastic distension (i.e., prestraining). If SFs were stretched and then anchored at their end points to a rigid substrate, their prestrain would be ε_0. Since they are anchored to a deformable substrate, then ε_0 is reduced by strain ε due to distortion of the substrate caused by the pulling action of the fiber prestress σ. Thus, the net fiber strain is $\varepsilon_0-\varepsilon$. The total potential energy (U_{SF}) of the SF is

$$U_{\mathrm{SF}} = W(\varepsilon_0-\varepsilon) - \sigma \times (\varepsilon_0-\varepsilon), \tag{1}$$

where $W(\cdot)$ is a strain energy function per unit resting volume (V_0) of the SF. Biomechanical measurements on isolated SFs show that under tension they exhibit stiffening such that their stiffness increases from 1.45 MPa at zero strain, to 109 MPa at the maximal (breaking) strain of ~200% (Deguchi et al., 2006). Thus, we assume $W(\cdot)$ to be of the following form:

$$W = \frac{1}{2}a_1(\varepsilon_0-\varepsilon)^2 + \frac{1}{4}a_2(\varepsilon_0-\varepsilon)^4, \tag{2}$$

where a_1 and a_2 are material constants. From the experimental stress–strain curves for SFs, we estimate that $a_1 = 1.45$ MPa and $a_2 = 9$ MPa.

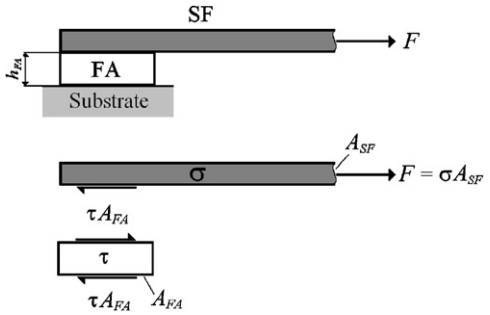

Fig. 1. A schematic depiction of a stress fiber (SF), focal adhesion (FA) and substrate interaction (top) and the corresponding free-body diagram (bottom). h_{FA} is the height of the FA; F is the pulling force exerted by the SF on the FA; σ is the corresponding stress in the SF and A_{SF} is the cross-sectional area of the SF; τ is the stress within the FA produced by F; A_{FA} is the contact area over which F is transmitted to the FA and also the contact area between the FA and the substrate; τA_{FA} is the force transmitted by the FA to the substrate.

2.2. Focal adhesions

Shemesh et al. (2005) described FAs as a molecular aggregate subjected to a pulling contractile force (F) which alters their chemical potential. Assuming that the stiffness of the FA aggregate is much greater than the magnitude of the stress (τ) within the aggregate produced by F, and that τ is uniformly distributed, the chemical potential (Ψ) per unit volume (v_0) of the aggregate can be described by the following relationship:

$$\Psi = \Psi_0 - \tau, \tag{3}$$

where Ψ_0 is the chemical potential per unit volume in the absence of the pulling force. In our model, F is provided by σ (Fig. 1).

3. Stability analysis

We define the total potential (U) of our model as follows:

$$U(\varepsilon) = nU_{\mathrm{SF}}(\varepsilon) + 2\phi n(\Psi_0 - \tau), \tag{4}$$

where n is the total number of SFs, $2n$ is the total number of FAs and $\phi = v_0/V_0$. Since U attains minimum at equilibrium, $\partial U/\partial\varepsilon = 0$ and it follows from Eqs. (1) and (4) that

$$\frac{\partial U}{\partial \varepsilon} = n\left(\frac{\partial W}{\partial \varepsilon} + \sigma\right) = 0. \tag{5}$$

By combining Eqs. (2) and (5), we obtain that

$$\sigma = a_1(\varepsilon_0-\varepsilon) + a_2(\varepsilon_0-\varepsilon)^3. \tag{6}$$

Since τ is generated by the pulling action of σ, it follows that $\sigma = \phi_A \tau$, where ϕ_A is a scaling factor that accounts for the difference in the cross-sectional area of the SF (A_{SF}) and the area of FA (A_{FA}) over which the pulling force is transmitted, i.e., $\phi_A = A_{FA}/A_{SF}$ (Fig. 1). Furthermore, $\phi = \phi_L \phi_A$, where ϕ_L is the ratio of the average height of the FA (h_{FA}) and the undeformed length of the SF (L_{SF}), i.e., $\phi_L = h_{FA}/L_{SF}$. Thus,

$$\phi\tau = \phi_L \phi_A \tau = \phi_L \sigma. \tag{7}$$

By combining Eqs. (1), (2), (4), (6) and (7), we obtain

$$\begin{aligned} U = & -n\left[\frac{1}{2}a_1(\varepsilon_0-\varepsilon)^2 + \frac{3}{4}a_2(\varepsilon_0-\varepsilon)^4\right] \\ & + 2n\{\phi\Psi_0 - \phi_L[a_1(\varepsilon_0-\varepsilon) + a_2(\varepsilon_0-\varepsilon)^3]\}. \end{aligned} \tag{8}$$

We assume that $\varepsilon < \varepsilon_0$, i.e., that SFs are under tension all the time.

We first consider the case where the substrate is divided into two regions, S_1 and S_2, of different stiffness with a clearly defined boundary that separates them, like in the experiments of Lo et al. (2000). Suppose that initially the fiber system is entirely anchored to the soft region of the substrate, say S_1. The corresponding $\varepsilon = \varepsilon_1$. By substituting ε_1 into Eq. (8), we obtain the total potential $U_1 \equiv U(\varepsilon_1)$. Consider a cell that migrates from S_1 to the stiffer region of the substrate, S_2. When the cell comes near the boundary that separates S_1 and S_2, it protrudes a lamellipodium across the boundary to probe stiffness of S_2. In our model, we mimic this as if $i < n$ ($i \geqslant 1$) SFs extend across the boundary and anchor only one of their FAs to S_2, while their other FAs remain anchored to S_1. Since S_2 is stiffer than S_1, the strain in the i protruding SFs becomes $\varepsilon_0 - \varepsilon_{1,2}$, where $\varepsilon_{1,2} < \varepsilon_1$, while in the remaining $(n-i)$ SFs the strain remains unaltered, i.e., $\varepsilon_0 - \varepsilon_1$. The corresponding total potential, $\bar{U}_1$, is

$$\begin{aligned} \bar{U}_1 \equiv U(\varepsilon_1, \varepsilon_{1,2}) = & (n-i)U_{SF}(\varepsilon_1) + iU_{SF}(\varepsilon_{1,2}) \\ & + 2\phi[n\Psi_0 - (n-i)\tau_1 - i\tau_{1,2}]. \end{aligned} \tag{9}$$

Equilibrium demands that $\partial\bar{U}_1/\partial\varepsilon_1 = 0$ and $\partial\bar{U}_1/\partial\varepsilon_{1,2} = 0$. Taking this into account and following the same steps as in Eqs. (5)–(7), we obtain from Eq. (9) that

$$\begin{aligned} \bar{U}_1 = & -(n-i)\left[\tfrac{1}{2}a_1(\varepsilon_0-\varepsilon_1)^2 + \tfrac{3}{4}a_2(\varepsilon_0-\varepsilon_1)^4\right] \\ & - i\left[\tfrac{1}{2}a_1(\varepsilon_0-\varepsilon_{1,2})^2 + \tfrac{3}{4}a_2(\varepsilon_0-\varepsilon_{1,2})^4\right] \\ & + 2\{n\phi\Psi_0 - (n-i)\phi_L[a_1(\varepsilon_0-\varepsilon_1) + a_2(\varepsilon_0-\varepsilon_1)^3] \\ & - i\phi_L[a_1(\varepsilon_0-\varepsilon_{1,2}) + a_2(\varepsilon_0-\varepsilon_{1,2})^3]\}. \end{aligned} \tag{10}$$

We then apply a global (Maxwell's) stability criterion to the model (cf. Ericksen, 1991). According to this criterion, an elastic system assumes a stable equilibrium configuration where the total potential attains its global minimum. By comparing U_1 and $\bar{U}_1$ (Eq. (10)) and taking into account that $\varepsilon_{1,2} < \varepsilon_1 < \varepsilon_0$, we obtain that $\bar{U}_1 < U_1$ and thus, by the global stability criterion, the configuration corresponding to $\bar{U}_1$ is more stable than the one corresponding to U_1. Thus, the cell will favor migration from S_1 towards S_2.

As the cell migration across the boundary between S_1 and S_2 progresses, at some point k SFs become anchored to S_2, m SFs to both S_1 and S_2, and $(n–m–k)$ SFs remain anchored to S_1, where $i < m < n$, $k < n$. The corresponding total potential, $U_{1,2}$, is given as follows:

$$\begin{aligned} U_{1,2} \equiv U(\varepsilon_1, \varepsilon_{1,2}, \varepsilon_2) = & (n-m-k)U_{SF}(\varepsilon_1) \\ & + mU_{SF}(\varepsilon_{1,2}) + kU_{SF}(\varepsilon_2) \\ & + 2\phi[n\Psi_0 - (n-m-k)\tau_1 - m\tau_{1,2} - k\tau_2], \end{aligned} \tag{11}$$

where $\varepsilon_2 < \varepsilon_{1,2} < \varepsilon_1$ and the strain in the m SFs that are anchored to S_2 becomes $\varepsilon_0 - \varepsilon_2$. Equilibrium demands that $\partial U_{1,2}/\partial\varepsilon_1 = 0$, $\partial U_{1,2}/\partial\varepsilon_{1,2} = 0$, and $\partial U_{1,2}/\partial\varepsilon_2 = 0$. Taking this into account and following the same steps as in Eqs. (5)–(7), we obtain from Eq. (11) that

$$\begin{aligned} U_{1,2} = & -(n-m-k)\left[\tfrac{1}{2}a_1(\varepsilon_0-\varepsilon_1)^2 + \tfrac{3}{4}a_2(\varepsilon_0-\varepsilon_1)^4\right] \\ & - m\left[\tfrac{1}{2}a_1(\varepsilon_0-\varepsilon_{1,2})^2 + \tfrac{3}{4}a_2(\varepsilon_0-\varepsilon_{1,2})^4\right] \\ & - k\left[\tfrac{1}{2}a_1(\varepsilon_0-\varepsilon_2)^2 + \tfrac{3}{4}a_2(\varepsilon_0-\varepsilon_2)^4\right] \\ & + 2\{n\phi\,\Psi_0 - (n-m-k)\phi_L[a_1(\varepsilon_0-\varepsilon_1) \\ & + a_2(\varepsilon_0-\varepsilon_1)^3] - m\phi_L[a_1(\varepsilon_0-\varepsilon_{1,2}) \\ & + a_2(\varepsilon_0-\varepsilon_{1,2})^3] - k\phi_L[a_1(\varepsilon_0-\varepsilon_2) \\ & + a_2(\varepsilon_0-\varepsilon_2)^3]\}. \end{aligned} \tag{12}$$

By comparing $U_{1,2}$ (Eq. (12)) and $\bar{U}_1$ (Eq. (10)), and taking into account that $\varepsilon_2 < \varepsilon_{1,2} < \varepsilon_1 < \varepsilon_0$, we obtain that $U_{1,2} < \bar{U}_1$ and thus, by the global stability criterion, the configuration corresponding to $U_{1,2}$ is more stable than the one corresponding to $\bar{U}_1$. Thus the cell will still favor migrating towards S_2.

Finally, the entire cell crosses the boundary between S_1 and S_2 such that all n SFs are completely anchored to S_2. Using the same steps as above, we obtain the corresponding total potential, U_2, as follows:

$$U_2 \equiv U(\varepsilon_2) = nU_{SF}(\varepsilon_2) + 2\phi n(\Psi_0 - \tau_2). \tag{13}$$

Using the equilibrium requirements $\partial U_2/\partial\varepsilon_2 = 0$ and the steps from Eqs. (5)–(7), we obtain from Eq. (13) the same expression as Eq. (8) with ε_2 replacing ε. By comparing U_2 and $U_{1,2}$ (Eq. (12)) and taking into account that $\varepsilon_2 < \varepsilon_{1,2} < \varepsilon_1 < \varepsilon_0$, we obtain that $U_2 < U_{1,2}$ and thus, by the global stability criterion, the configuration corresponding to U_2 is more stable than the one corresponding to $U_{1,2}$. Thus the cell will still favor migrating towards S_2.

Consider now migration from S_2 towards S_1. When the cell comes close to the boundary that separates S_1 and S_2, it will protrude a lamellipodium across the boundary to probe stiffness of S_1. Then, following the same procedure as in Eqs. (9) and (10), we obtain the total potential $\bar{U}_2 \equiv U(\varepsilon_2, \varepsilon_{1,2})$ of the same form as Eq. (10), with ε_2 replacing ε_1. By comparing $\bar{U}_2$ and U_2 and taking into account that $\varepsilon_2 < \varepsilon_{1,2}$, we obtain that $U_2 < \bar{U}_2$ and therefore, by the Maxwell's global stability criterion, the configuration corresponding to U_2 is more stable than the one

corresponding to $\bar{U}_2$. Thus, the cell would tend to remain anchored to S_2.

We next consider the case where substrate stiffness (E_s) continuously increases in one direction, like in the experimental study of Wong et al. (2003). In that case, strain ε will continuously decrease with increasing E_s, i.e. $d\varepsilon/dE_s<0$. Thus by taking the derivative of U (Eq. (8)) with respect E_s, we obtain

$$\frac{dU}{dE_s} = n[2\phi_L a_1 + a_1(\varepsilon_0-\varepsilon) + 6\phi_L a_2(\varepsilon_0-\varepsilon)^2 + 3a_2(\varepsilon_0-\varepsilon)^3]\frac{d\varepsilon}{dE_s}. \quad (14)$$

Since all terms in the angular parentheses on the right-hand side of Eq. (14) are positive, it follows that $dU/dE_s<0$, since $d\varepsilon/dE_s<0$, and therefore U decreases with increasing E_s. According to Maxwell's criterion, decreasing U implies that stability increases. Thus, the cell will tend to migrate from the softer towards the stiffer region of the substrate and not in the opposite direction, which is consistent with experimental observations (Wong et al., 2003).

4. Numerical results

To obtain quantitative values of the total potential, we first estimate the model parameters using data from the literature as follows: Balaban et al. (2001) measured that the force exerted on a single FA is $F = 10\,\text{nN}$ and the corresponding constant stress within the FA is $\tau = 5.5\,\text{kPa}$. Since the cross-sectional radius of SFs is $r \approx 100\,\text{nm}$ (Deguchi et al., 2006), we obtain the corresponding $\sigma = F/\pi r^2 = 320\,\text{kPa}$ (Fig. 1). From this value of σ and experimental data for stress–strain behavior of individual SFs (Deguchi et al., 2006), we obtain that $\varepsilon_0 = 0.22$.

To calculate strain ε due to the compliance of the substrate, we assume that a SF and the substrate are like springs mechanically in series, i.e., two substrate springs of undeformed length L_s attached to each end of the SF spring of undeformed length L_{SF}, with the other ends of the substrate springs held fixed. The SF spring is prestrained to $\varepsilon_0 = 0.22$, and the corresponding force in the spring is $F = 10\,\text{nN}$, prior to being connected to the two substrate springs. By considering equilibrium of this system, we obtain ε as follows:

$$\varepsilon = \frac{2\varepsilon_0}{2 + \frac{E_s}{E_{SF}\phi_A}\frac{L_{SF}}{L_s}}, \quad (15)$$

where E_s and E_{SF} are the elastic moduli of the substrate and the SF, respectively. To estimate ϕ_A, we use Eq. (7) and obtain that $\phi_A = \sigma/\tau = 320/5.5 = 58.2$. We choose *ad hoc* $L_{SF} = 20\,\mu\text{m}$ and $L_s = 1\,\mu\text{m}$. $E_{SF} = 1.45\,\text{MPa}$ is obtained from the experimental data of Deguchi et al. (2006). Using the values for E_s of 14 kPa for S_1 and 30 kPa for S_2, as in the experiments of Lo et al. (2000), we calculate $\varepsilon_1 = 0.037$ and $\varepsilon_2 = 0.017$. We chose *ad hoc* $\varepsilon_{1,2} = 0.027$.

To estimate ϕ_L, we assume that the average FA thickness is approximately equal to the diameter of the SF, i.e., $h_{FA} = 0.2\,\mu\text{m}$. Thus, $\phi_L = h_{FA}/L_{SF} = 0.01$.

We do not have experimentally based estimates for Ψ_0. However, since in our model Ψ_0 is an additive constant to the total potential, it has no effect on changes of the potential and thereby on stability.

To complete our calculations, we assign the following arbitrary values to the number of elements, $n = 100$, $m = k = 33$, $i = 10$.

Using the above parameter values, we first calculate U_1, $\bar{U}_1$, $U_{1,2}$, U_2 and $\bar{U}_2$ from Eqs. (8), (10) and (12). A schematic depiction of cell migration from S_1 to S_2 shows how the total potential decreases as the cell crosses the boundary between S_1 and S_2 (Fig. 2). This gaining of stability in the direction of increasing substrate stiffness is consistent with the direction of cell migration (Lo et al., 2000). Migration in the opposite direction, from S_2 and S_1, leads to an increase in the total potential, stability loss, and thus the cell will not migrate in this direction (Fig. 2), consistent with the experimental observations (Lo et al., 2000).

In the case of gradient stiffness substrates, we obtain a relationship between U and E_s as follows. We use data from the study of Wong et al. (2003), where cells were cultured on 9-mm radius (R) circular substrates whose stiffness gradually increased in the radial direction, from 2.5 kPa near the perimeter of the circle to 11.5 kPa near its center. Assuming a linear dependence between E_s and R,

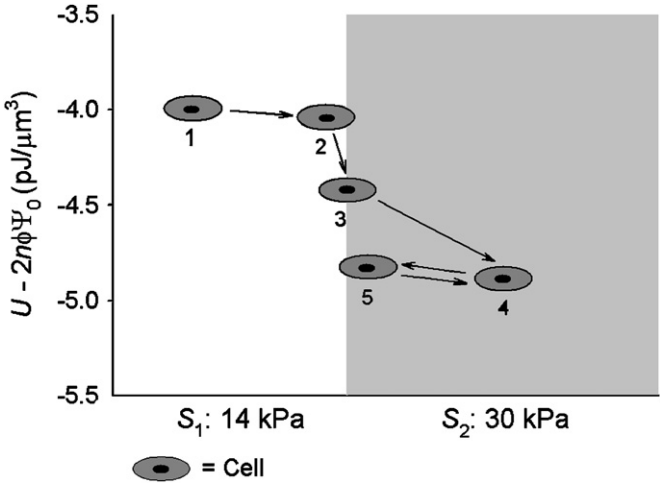

Fig. 2. Numeric simulations of changes in the total potential ($U-2n\phi\Psi_0$) of the model as the cell migrates from the soft substrate region S_1 (stiffness $E_s = 14\,\text{kPa}$) to the stiff substrate region S_2 ($E_s = 30\,\text{kPa}$); $2n\phi\Psi_0$ is a constant that indicates the chemical potential of focal adhesions (FAs) in the absence of pulling force. As the cell moves from S_1 to S_2, $U-2n\phi\Psi_0$ decreases and the cell gains stability until it completely crosses the boundary that separates S_1 from S_2. Thus cell will favor migration from the softer to the stiffer substrate region. If the cell tends to migrate from S_2 to S_1, $U-2n\phi\Psi_0$ will increase and the cell will lose stability. Thus, the cell will not favor migration from the stiffer to the softer substrate region. The arrows indicate the direction of migration. These results are consistent with experimental observations (Lo et al., 2000).

we obtain $E_s = 2.5 + R$ in kPa. By substituting this relationship into Eq. (15), we obtain ε as a function of R. By substituting such obtained ε vs. R relationships into Eq. (8), we obtain a U vs. R relationship. By cross-plotting the U vs. R and the E_s vs. R relationships, we obtain a U vs. E_s relationship (Fig. 3). We find that U decreases with increasing E_s, indicating that the model gains stability in the direction of increasing substrate stiffness, which is consistent with the observed direction of cell migration (Wong et al., 2003).

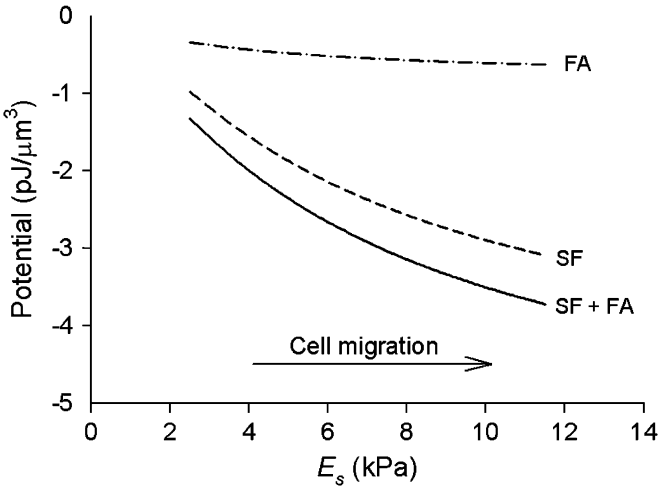

Fig. 3. The total potential of decreases with increasing substrate stiffness (E_s) indicating that stability also increases; FA (dash-dot-dash curve) indicates the contribution of focal adhesions; SF (dashed curve) indicates the contribution of stress fibers; and SF + FA (solid curve) indicates the contribution of both. The calculations are carried out based on Eq. (8), not including the constant $2n\phi\Psi_0$, indicative of the chemical potential of FAs in the absence of pulling force. The decrease of the total potential is consistent with experimental data on substrates with gradient stiffness which show that cells migrate in the direction of increasing E_s (indicated by the arrow) and not in the opposite direction (Wong et al., 2003).

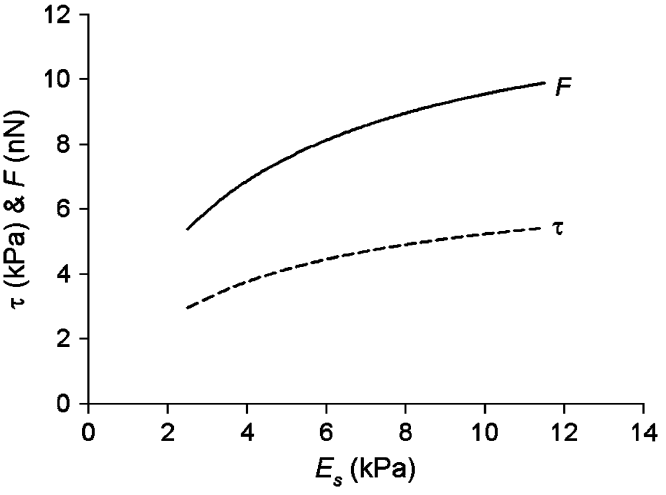

Fig. 4. Pulling force (F) of the stress fiber produces stress (τ) within the focal adhesion. The model predicts that both F (solid line) and τ (dashed line) increase with increasing substrate stiffness (E_s). Quantitatively, these predictions are consistent with experimental data from living cells (Balaban et al., 2001).

We also calculate the relative contributions of SFs and FAs to U and how these contributions depend on E_s (Fig. 3). We find that both the elastic potential of SFs and the chemical potential of FAs decrease with increasing E_s and that the contribution of SFs is predominant (Fig. 3). The decrease in the chemical potential with increasing E_s results from the increasing FA stress τ (Eq. (5)), generated by the pulling force F of SFs (Fig. 4). Importantly, the predicted values of τ and F (Fig. 4) fall in the range of experimentally measured values (Balaban et al., 2001).

5. Discussion

We propose a mathematical model that describes durotaxis as a stability phenomenon. According to the model, the stiffer the substrate, the greater the stability of SFs and FAs. Since stable configurations are energetically less costly, they would increase the cell's functional efficiency and therefore cells would favor more stable over less stable configurations. Consequently, on a substrate of variable stiffness this preference for a stable configuration would result into a directional cell motion from softer towards stiffer regions.

The model shows that elasticity of the actin network is a dominant stabilizing mechanism during durotaxis, whereas the strengthening of FAs appears to have a relatively minor contribution. This is a novel finding since in previous studies strengthening of FAs via contractile forces has been viewed as a key stabilizing mechanism (Pelham and Wang, 1997; Sheetz et al., 1998; Lo et al., 2000; Discher et al., 2005; Jiang et al., 2006).

There are a number of simplified and *ad hoc* assumptions in the model, including the assumed uniformity of geometry, material properties, structural organization and prestress distribution as well as the dimensionality of the network. For example, uniform prestress distribution of SFs implies that the cell remains under uniform mechanical distension during durotaxis, and thus microstructural geometry and its connectedness need not be specified. This certainly is not the case since the cell alters its shape as it migrates. To account for the shape distortion, interconnectedness and structural geometry of the network are needed. While this would certainly affect the stability analysis, we believe that the outcome would be the same as in the present model, i.e., that with increasing substrate stiffness the model would gain stability.

We omit the potential contribution of other CSK components, especially microtubules that are essential for cell migration. Microtubules provide polarity to migrating cells, and in that process they mechanically interact with the actin CSK in the base of lamellipoda. This is indicated by their buckling as they exert push against the contractile actin (Waterman-Storer and Salmon, 1999). If we view microtubules as compression-supporting elements that resist contraction of the actin network, then one would expect their elastic potential to increase with increasing substrate stiffness, since the resistance to the contractile stress would be increasingly provided by FAs (Hu et al., 2004). This, in turn,

implies that microtubules would have a destabilizing effect during durotaxis. When we include the contribution of microtubules into our model and then carry out the stability analysis, we find that their destabilizing effect is minor in comparison to the stabilizing effect of SFs. In order to maintain mathematical clarity and transparency, we omit the contribution of microtubules from the model.

While our model may be reasonable for describing durotaxis in two-dimensional cell cultures, where SFs are prominent and FAs are discrete entities, it may not be appropriate for three-dimensional cell cultures which often lack SFs and discrete FAs (Grinnell et al., 2003; Friedl and Bröcker, 2000). On the other hand, experimental studies of durotaxis were carried out in two-dimensional cultures (Lo et al., 2000; Wong et al., 2003) and therefore, our model seems to be a good approach for two-dimensional cultures.

Model parameters are estimated based on experimental data from the literature. In the absence of experimental data, some parameter values are chosen *ad hoc*, like the length of SFs and dimensions of FAs. Despite this arbitrariness, the quantitative predictions of the model (Fig. 4) are consistent with measurements in living cells, suggesting that the selected parameter values are reasonable.

We have used previously a similar stability analysis to study cell reorientation in response to static substrate stretching (Lazopoulos and Stamenović, 2006; Lazopoulos and Pirentis, 2007). We have shown that cells tend to orient either parallel with or away from the direction of the principal substrate strain, depending on the level of SF prestrain and on their constitutive properties. It is feasible that a similar approach can be used to study cellular response to substrate material anisotropy. Using a minimum contractile work argument, Bischofs and Schwarz (2003) showed that cells would always align with the direction of the maximal substrate stiffness, which is consistent with experimental data (Saez et al., 2007).

In summary, despite its simplicity and limitations, our model provides a physically plausible and mathematically transparent explanation of durotaxis as an elastic stability phenomenon. It shows that the elastic stability of SFs is a major stabilizing factor during durotaxis. This model can be used in future investigations of various types of cell mechanosensing phenomena.

Conflict of interest statement

The work presented here does not involve any conflict of interest. The work was not funded by any governmental or private foundations and grants. The salary support for the authors was provided by the National Technical University of Athens and Boston University.

References

Balaban, N.Q., Schwarz, U.S., Riveline, D., Goichberg, P., Tzur, G., Sabanay, I., Mahalu, D., Safran, S., Bershadsky, A., Addadi, L., Geiger, B., 2001. Force and focal adhesion assembly: a close relationship studied using elastic micropatterned substrates. Nature Cell Biology 3, 466–472.

Bischofs, I.B., Schwarz, U.S., 2003. Cell organization in soft media due to active mechanosensing. Proceedings of the National Academy of Sciences of the USA 100, 9274–9279.

Deguchi, S., Ohashi, S., Sato, M., 2006. Tensile properties of single stress fibers isolated from cultured vascular smooth muscle cells. Journal of Biomechanics 39, 2603–2610.

Discher, D.E., Janmey, P., Wang, Y.-l., 2005. Tissue cells feel and respond to the stiffness of their substrate. Science 310, 1139–1143.

Ericksen, J.L., 1991. In: Knops, R.J., Morton, K.W. (Eds.), Introduction to the Thermodynamics of Solids. Chapman & Hall, London, pp. 39–61 (Chapter 3).

Friedl, P., Bröcker, E.-B., 2000. The biology of cell locomotion within three-dimensional extracellular matrix. Cellular and Molecular Life Sciences 57, 41–64.

Grinnell, F., Ho, C.-H., Tamariz, E., Lee, D.J., Skuta, G., 2003. Dendritic fibroblasts in three-dimensional collagen matrices. Molecular Biology of the Cell 14, 384–395.

Hu, S., Chen, J., Wang, N., 2004. Cell spreading controls balance of prestress by microtubules and extracellular matrix. Frontiers in Bioscience 9, 2177–2182.

Jiang, G., Huang, A.H., Cai, Y., Tanse, M., Sheetz, M.P., 2006. Rigidity sensing at the leading edge through $\alpha_v\beta_3$ integrins and RPTPα. Biophysical Journal 90, 1804–1809.

Lazopoulos, K.A., Pirentis, A., 2007. Substrate stretching and reorganization of stress fibers as a finite elasticity problem. International Journal of Solids and Structures 44, 8285–8296.

Lazopoulos, K.A., Stamenović, D., 2006. A mathematical model of cell reorientation in response to substrate stretching. Molecular & Cellular Biomechanics 3, 43–48.

Li, S., Guan, J.-L., Chien, S., 2005. Biochemistry and biomechanics of cell motility. Annual Review of Biomedical Engineering 7, 105–150.

Lo, C-M., Wang, H-B., Dembo, M., Wang, Y-l., 2000. Cell movement is guided by the rigidity of the substrate. Biophysical Journal 79, 144–152.

Mitchison, T.J., Cramer, L.P., 1996. Actin-based cell motility and cell locomotion. Cell 84, 371–379.

Pelham Jr., R.J., Wang, Y.-l., 1997. Cell locomotion and focal adhesions are regulated by substrate flexibility. Proceedings of National Academy of Sciences of the United States of America 94, 13661–13665.

Ridley, A.J., Schwartz, M.A., Burridge, K., Firtel, R.A., Ginsberg, M.H., Borisy, G., Parsons, J.T., Horwitz, A.R., 2003. Cell migration: integrating signals from front to back. Science 302, 1704–1709.

Saez, A., Ghibaudo, M., Buguin, A., Silberzan, P., Ladoux, B., 2007. Rigidity-driven growth and migration of epithelial cells on microstructured anisotropic substrate. Proceedings of the National Academy of Sciences of the USA 104, 8281–8286.

Sheetz, M.P., Felsenfeld, D.P., Galbraith, C.G., 1998. Cell migration: regulation of force on extracellular matrix-integrin complexes. Trends in Cell Biology 8, 51–54.

Shemesh, T., Geiger, B., Bershadsky, A.D., Kozlov, M.M., 2005. Focal adhesions as mechanosensors: a physical mechanism. Proceedings of National Academy of Sciences of the United States of America 102, 12383–12388.

Wang, J.H.-C., 2000. Substrate deformation determines actin cytoskeleton reorganization: mathematical modeling and experimental study. Journal of Theoretical Biology 202, 33–41.

Wang, N., Naruse, K., Stamenović, D., Fredberg, J.J., Mijailovich, S.M., Tolić-Nørrelykke, I.M., Polte, T., Mannix, R., Ingber, D.E., 2001. Mechanical behavior in living cells consistent with the tensegrity model. Proceedings of National Academy of Sciences of the United States of America 98, 7765–7770.

Waterman-Storer, C.M., Salmon, E.D., 1999. Positive feedback interactions between microtubules and actin dynamics during cell motility. Current Opinion in Cell Biology 11, 61–67.

Wong, J.Y., Velasco, A., Rajagopalan, P., Pham, Q., 2003. Directed movement of vascular smooth muscle cells on gradient compliant hydrogels. Langmuir 19, 1908–1913.